Journal of Anatomy

J. Anat. (2019) **234**, pp637–655 doi: 10.1111/joa.12952

The bizarre skull of *Xenotyphlops* sheds light on synapomorphies of Typhlopoidea

Johann Chretien,[1] Cynthia Y. Wang-Claypool,[2] Frank Glaw[1] and Mark D. Scherz[1,3]

[1]*Zoologische Staatssammlung München (ZSM-SNSB), Munich, Germany*
[2]*Museum of Vertebrate Zoology, University of California, Berkeley, CA, USA*
[3]*Zoologisches Institut, Technische Universität Braunschweig, Braunschweig, Germany*

Abstract

The emerging picture of non-monophyly of scolecophidian snakes is increasingly indicative that fossorial lifestyle, myrmecophagous diet, and miniaturisation are powerful drivers of morphological evolution in squamate skulls. We provide a detailed description of the skull of *Xenotyphlops grandidieri*, with reference to the skulls of other scolecophidian snakes. The skull, which shows dramatic ventral inflection of the snout complex, is remarkably bizarre, and the mouth opening is more ventrally oriented than in other typhlopoids. The eyes are strongly reduced, and the enlarged and rather flat anterior head shield is covered in numerous sensillae. We put forward several potential explanations for the evolution of these unusual modifications. On the other hand, *Xenotyphlops* shares numerous synapomorphies with other typhlopoid snakes, including the highly specialized jaw mechanism. We argue that the key differences between the jaw mechanisms of Leptotyphlopidae, Anomalepididae, and Typhlopoidea provide compelling evidence for a strong role of convergence in the evolution of the scolecophidian bauplan, and these clades therefore cannot be interpreted as representative of ancestral anatomy or ecology among snakes.

Key words: comparative morphology; osteology; Scolecophidia; Typhlopoidea; *Typhlops*; Xenotyphlopidae.

Highlight

The skull of the typhlopoid snake *Xenotyphlops grandidieri* is ventrally inflected, resulting in positional rearrangement of its snout bones and the formation of a robust anterior plate to the skull. It shares the unique rotational jaw mechanism seen in Gerrhopilidae and Typhlopidae, making this mechanism a synapomorphy of the superfamily Typhlopoidea. Differences in jaw morphology among major scolecophidian *sensu lato* lineages implicates convergent evolution in generating the blindsnake bauplan.

Introduction

Scolecophidians have long been considered an ancient radiation of snakes (reviewed in Burbrink & Crother, 2011), representing a specialization on burrowing that probably does not reflect the morphology of stem snakes but rather a derived, specialized morphology. The infraorder Scolecophidia *sensu lato* (see Miralles et al. 2018; Fig. 1) consists of five families: Typhlopidae, Gerrhopilidae, Xenotyphlopidae (together constituting the superfamily Typhlopoidea), Anomalepididae, and Leptotyphlopidae (Vidal et al. 2010). Most morphological studies have alleged numerous synapomorphic features of scolecophidians (List, 1966; Rieppel, 1988; Cundall et al. 1993; Lee & Scanlon, 2002), but others have warned against overinterpretation of character states that could also be convergences as synapomorphies (Cundall & Irish, 2008). Although some genetic studies have also supported the monophyly of the Scolecophidia (Macey & Verma, 1997; Vidal & Hedges, 2002; Lee et al. 2007), as has often and long been assumed (e.g. List, 1966; Rieppel, 1988; Vitt & Caldwell, 2009; Burbrink & Crother, 2011), the majority of recent studies do not (Forstner et al. 1995; Heise et al. 1995; Vidal & Hedges, 2005; Vidal et al. 2007, 2010; Wiens et al. 2008; Pyron et al. 2013a,b; Hsiang et al. 2015; Reeder et al. 2015; Figueroa et al. 2016; Zheng & Wiens, 2016; Harrington & Reeder, 2017; Streicher & Wiens, 2017; Miralles et al. 2018). The question of scolecophidian monophyly is therefore putatively resolved (Miralles et al. 2018), but the morphology of scolecophidian lineages must be reconciled in light of phylogenetic evidence.

Correspondence
Mark D. Scherz, Zoologische Staatssammlung München (ZSM-SNSB), Münchhausenstr. 21, 81247 Munich, Germany.
E: mark.scherz@gmail.com

Accepted for publication *11 January 2019*
Article published online *10 February 2019*

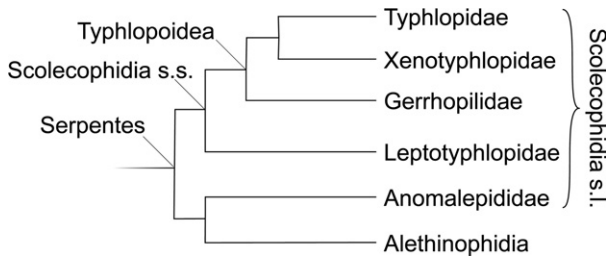

Fig. 1 A simplified phylogeny of the major lineages of Scolecophidia *sensu lato (s.l.)*, based on the latest phylogeny of Miralles et al. (2018).

Osteological work has shown remarkable diversity in skull architecture in Scolecophidia *sensu lato*, including major rearrangements of specific bones (e.g. those of the upper jaw), that lends support for an argument for the non-monophyly of this group, and indisputably supports extremely deep divergences among lineages (Cundall & Irish, 2008). Regrettably, no skull fossils are known from this group (Szyndlar, 1991; Mead, 2013), so our understanding of the evolution of their skull morphology must rest on studies of extant species in a robust phylogenetic framework. Although the relationships of the deep branches in the snake tree have not yet reached a point where they might be called 'robust', recent advances have promising support (Miralles et al. 2018).

The skulls of Leptotyphlopidae and Anomalepididae have been described in great detail, especially in Cundall & Irish (2008), Haas (1959, 1964), Rieppel (1979), and Rieppel et al. (2009). Of the typhlopoid families, detailed skull descriptions are only available for Typhlopidae (reviewed in Cundall & Irish, 2008), and a brief account of the osteology of one species of Gerrhopilidae (*Gerrhopilus persephone* Kraus, 2017) was recently published (Kraus, 2017). The skull of the third family in the superfamily Typhlopoidea, Xenotyphlopidae, was depicted in an X-ray by Wallach & Ineich (1996), but was not described, and so its remarkable morphology went understated. The family Xenotyphlopidae includes a single species, *Xenotyphlops grandidieri* (Mocquard, 1905) (Fig. 2I), endemic to a small coastal area in north Madagascar (Wegener et al. 2013), and was erected by Vidal et al. (2010) based on its phylogenetic position. To understand the evolution of skull morphology, it is critical to have detailed descriptions and high-resolution imagery or illustrations of the morphology of their skulls. In the present study, we contribute to this goal by describing the skull of *Xenotyphlops grandidieri* based on micro-computed tomography (micro-CT) data, allowing us to examine the minute skull of these snakes in intimate detail.

Materials and methods

The skulls of three specimens of *X. grandidieri* from the Zoologische Staatssammlung München (ZSM) in Germany (ZSM 2194/2007, ZSM 2216/2007, and ZSM 2213/2007) were micro-CT scanned using a phoenix|x nanotom m cone-beam scanner (GE Measurement & Control, Wunstorf, Germany). Scanning was performed using a tungsten target and a 0.1-mm Cu filter. Parameters were as follows: current 80 μA, voltage 110 kV, timing 750 ms, averaging 1, skip 0, 2440 projections, total scan time 30 min. Scan images were constructed into a volume file in DATOS|X RECONSTRUCT software (GE Measurement & Control), and imported as 8 bit into VG STUDIO MAX 2.2 (Volume Graphics GmbH, Heidelberg, Germany). The models were registered using the simple registration function. Each was then exported as an ANALYZE file, and a DICOM stack. The models of two of these specimens (ZSM 2216/2007 and ZSM 2213/2007) were included in Supporting Information Figs S1–S3.

A segmented 3D model of the skull of ZSM 2194/2007 was rendered in AMIRA 6.0 (Stalling et al. 2005): initially the skull was separated from the matrix using the threshold tool, and each bone was subsequently segmented manually using the brush tool. The segmented model was used to bound volume renderings of the skull in AMIRA to produce the figures in this paper. The model was smoothed to reduce artefacts, and each element was exported as an .obj file. These files were imported into ADOBE® 3D TOOLKIT (Adobe Systems Incorporated, San Jose, CA, USA), where the elements were recombined, simplified, and individually coloured. The resulting model was then exported as a .u3d file, embedded into a Portable Document File (PDF), and included in Figs S1–S3.

The DICOM stacks, rotational videos produced in VG STUDIO, and 3D models of the scans have been deposited on MorphoSource.org and are available from the following link: https://www.morphosource.org/Detail/ProjectDetail/Show/project_id/542.

The general form and each separate bone of the skull were precisely described based on the volume renderings of the segmented specimen skull following the recommendations of Scherz et al. (2017). The variation within the three skulls was investigated using the segmented model of ZSM 2194/2007, and the non-segmented models of ZSM 2216/2007 and ZSM 2213/2007. The chondrocranium is not described due to the low X-ray absorption of cartilage.

Results

The skull of *Xenotyphlops* (Fig. 2) is starkly different from all known skulls of the typhlopids and gerrhopilids but shares with them several features that differentiate these two families from the Leptotyphlopidae and Anomalepididae. In the following account, we describe each bone of the skull in detail, identifying, also characters that differ or resemble other members of the Scolecophidia in a meaningful manner.

General form

The skull is robust in form, and the bones are thick, creating strong sutures (Fig. 2). The posterior cranium is as broad as the snout complex, but narrows anteriorly until the middle of the frontals, before broadening suddenly once more. In lateral view (Fig. 2A), the shape of the skull is reminiscent of the beak of a flamingo, with the whole of the snout complex deflected downwards to sit almost beneath the anterior braincase. As a result of this deflection, structures of the snout are rotated by nearly 90° relative to those in

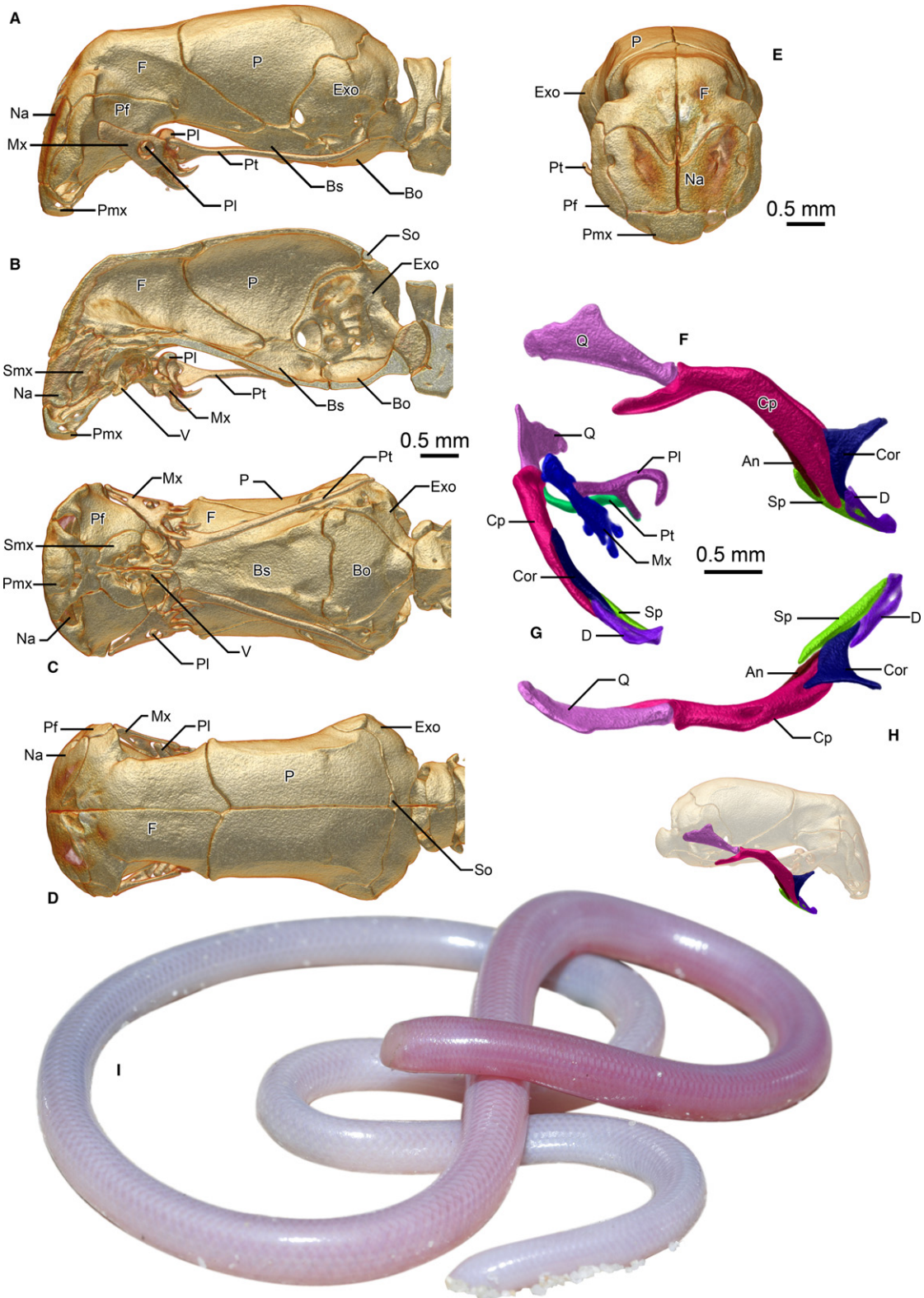

Fig. 2 Cranium and upper jaw (A–E) and lower jaw (F–H) of *Xenotyphlops grandidieri* in (A,F) lateral, (B) sagittal, (C) ventral, (D,H) dorsal, and (E,G) anterior view as well as an individual in life (I). An, angular; Bo, basioccipital; Bs, basisphenoid; Cor, coronoid; Cp, compound; D, dentary; Exo, exoccipital; F, frontal; Mx, maxilla; Na, nasal; P, parietal; Pf, prefrontal; Pl, palatine; Pmx, premaxilla; Pt, pterygoid; Q, quadrate; Smx, septomaxilla; So, supraoccipital; Sp, splenial; V, vomer.

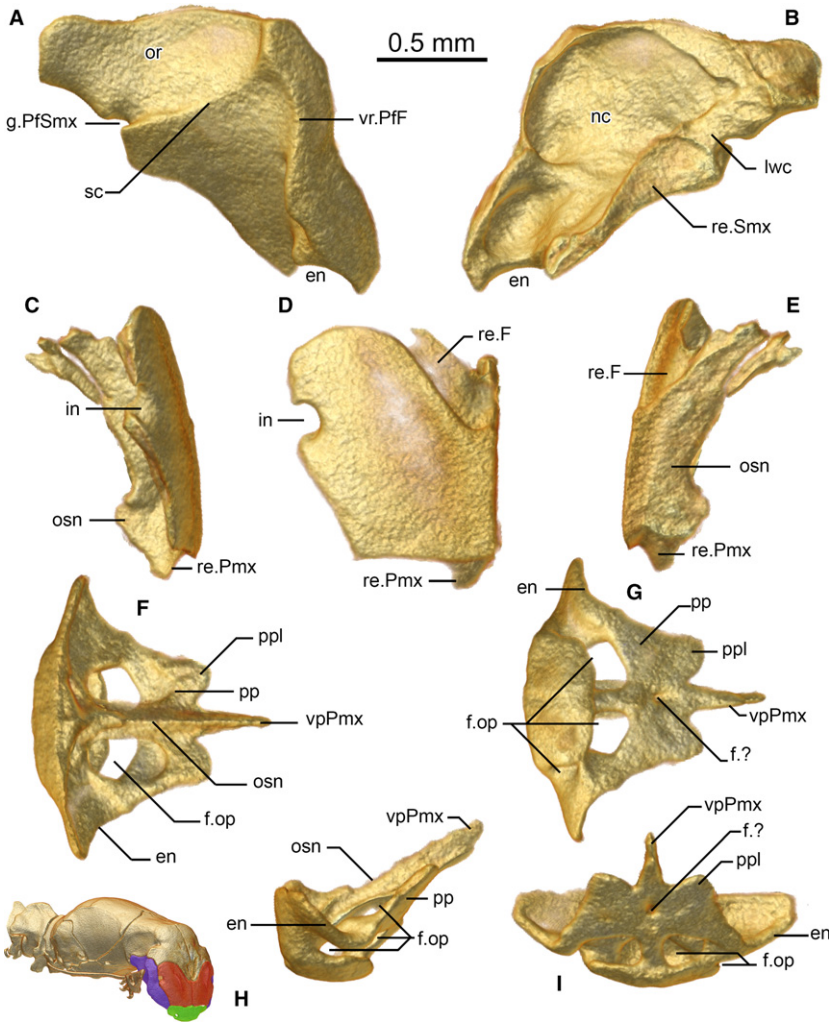

Fig. 3 Prefrontal (A,B), nasal (C–E), and premaxilla (F–I) of *Xenotyphlops grandidieri* in (A,C,H) lateral, (B,E) medial, (D) anterior, (I) posterior, (F) anterodorsal, and (G) posteroventral view. en, external naris; f.?, unknown foramen; f.op, foramen for the ophthalmus profundicus branch of trigeminal; g.PfSmx, prefrontal-septomaxillary groove of unknown function; in, invagination; lwc, lateral wall of choana; nc, nasal cavity, nostril; or, optic recession; osn, osseous septum nasi; pp, pars palatina; ppl, lobe of the pars palatina; re.F, receiving surface for frontal; re.Pmx, receiving surface for premaxilla; re.Smx, receiving surface for septomaxilla; sc, sigmoid crest of prefrontal; vpPmx, vomerine process of the premaxilla; vr.PfF, prefrontal-frontal vertical ridge.

typhlopoids, including the external naris (Fig. 2C), which is liable to make interpretation somewhat more complicated than it might otherwise be. Figures are here presented in analogous aspect, contextualised to their actual placement in the reference skull.

The skull is at its shallowest at the posterior-most level of the prefrontal-frontal suture, just anterior to the anterior-most extension of the parietals, where it is also roughly at its narrowest. The anterior wall of the skull, composed of the frontal, nasal, prefrontal, and premaxilla, is rather flat and reinforced, and slightly posteriorly angled.

The snout complex

The snout complex is composed of a single premaxilla, paired septomaxillae, paired but strongly fused vomers, paired nasals, and paired prefrontals [composition the same as in other typhlopoid species (Cundall & Irish, 2008; Kraus, 2017) except for the septomaxilla, which is fused anteriorly but posteriorly separated in *G. persephone* (Kraus, 2017), but this peculiarity might be an artefact created by the low definition of the micro-CT scan of this species; anomalepidids and leptotyphlopids have fused nasals (Rieppel et al. 2009; Figs 2–4)]. It shares with other typhlopoids the highly mobile maxillae, which are a chief difference to both Leptotyphlopidae and Anomalepididae (discussed in more detail below). Like other typhlopoids, the prefrontal bulges laterally but, unlike other members of the superfamily, it is displaced anteriorly to form the lateral face of the flattened snout (Figs 2E and 3A), and largely excludes the septomaxillae from the borders of the external naris.

Premaxilla

In anterior aspect, the premaxilla is a subtrapezoidal bone with a medial septum extending from its posterior border (Fig. 3F–I). It is edentulous, as in all scolecophidians *sensu lato*. The anterodorsal edge of the premaxilla is horizontal, with a slight dorsal projection at the midpoint between the nasals. This edge of the premaxilla is entirely in contact with the nasals dorsally, and its posterior face is also in contact with a posteromedial extension of each nasal on either side of the medial septum. Laterally, a squared corner to the

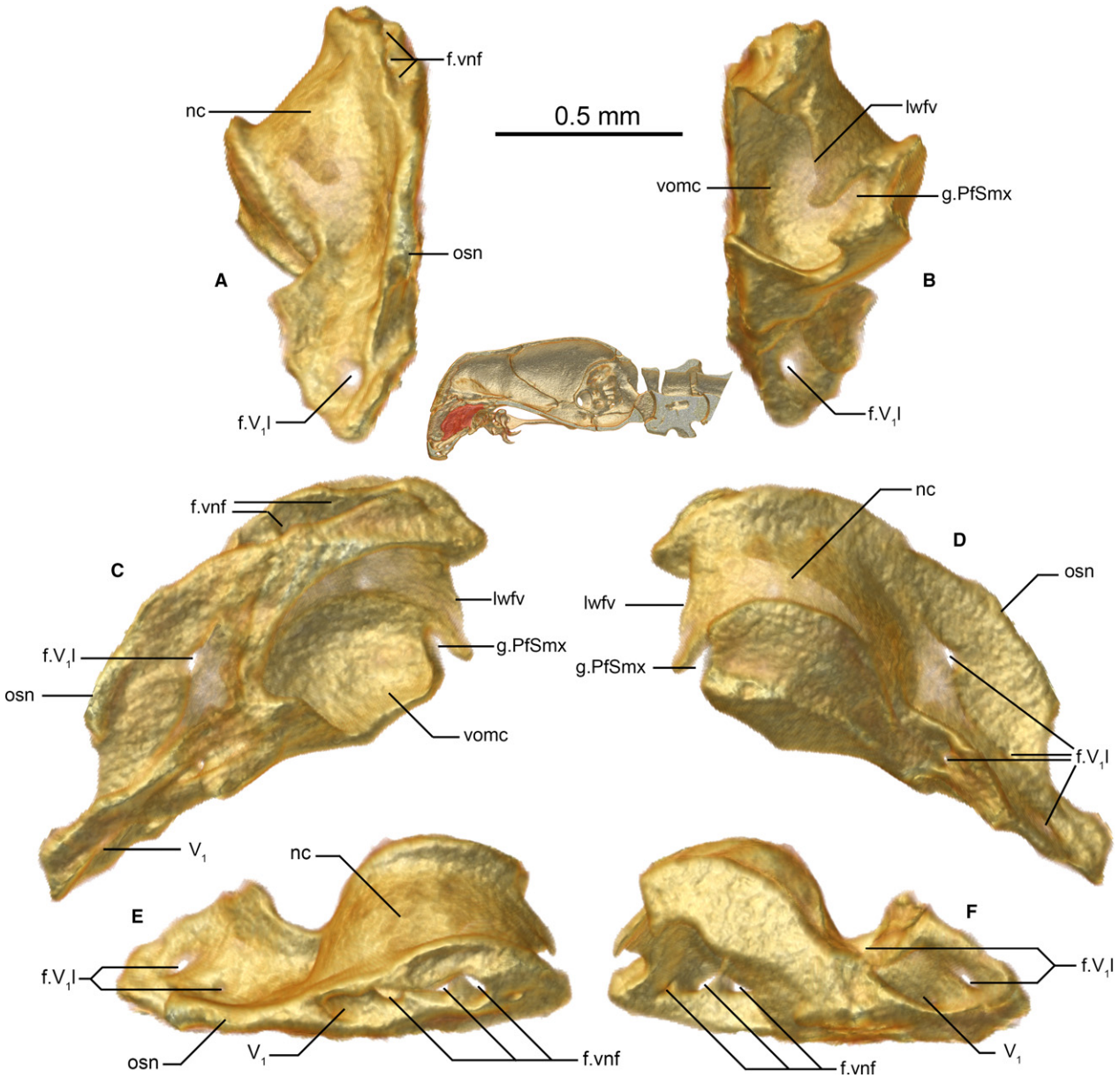

Fig. 4 Septomaxilla of *Xenotyphlops grandidieri* in (A) anterior, (B) posterior, (C) medial, (D) lateral, (E) dorsal, and (F) ventral view. f.V_1l, V_1 (trigeminal) lateral foramen; f.vnf, vomeronasal foramen/ina of the septomaxilla; g.PfSmx, prefrontal-septomaxillary groove of unknown function; lwfv, lateral wall of the fenestra vomeronasalis; nc, nasal cavity, nostril; osn, osseous septum nasi; V_1, trigeminal; vomc, vomeronasal cupola.

anterior face is present, at the junction between the nasals and the prefrontals. This edge confines the nasals entirely to the anterior face of the skull, and excludes them from participation in the external naris. The naris is formed solely by the prefrontals and the premaxilla with a small internal participation by the septomaxilla, a state that differs from all known typhlopoids, where the nasal participates in the external naris (Cundall & Irish, 2008), and the septomaxilla forms a considerable portion of the posterior edge of the naris (Palci et al. 2016; Kraus, 2017). A ventral lobe of the premaxilla is formed by the presence of four large foramina oriented posteroventrally (Fig. 3I); these are asymmetrical in ZSM 2194/2007, being separated by a small bony strut on the right side, and entirely connected on the left (i.e. three foramina; Fig. 3G), but presumably this is a growth defect, as the two other scanned *Xenotyphlops* specimens as well as all other scolecophidians have four (Rieppel et al. 2009). Haas (1964) showed that these foramina are responsible for transporting the ophthalmicus profundus (V_1) nerve, but they may also transmit a vein from the tip of the snout to the maxillary vein (McDowell, 2008). The openings enter into the ventral extension of the septomaxillae, which overlap the entire posterior component of the premaxilla. A low medial septum (Fig. 3H) of the premaxilla runs from

the anterior wall posterodorsally to the vomerine process, separating the septomaxillae from one another posteriorly. This septum forms a connection between the ventromedial bulb of the premaxilla and the dorsal surface of the pars palatina on either side of the medial septum of the premaxilla. The septum continues as the anterodorsal component of the acuminate vomerine process, which passes between the septomaxillae, and infiltrates the anteroventral vomer. This structure is similar to that of *Typhlops jamaicensis* (Shaw, 1802), but the septum is much lower than in that species (Rieppel et al. 2009). The pars palatina also possesses two weak lateral lobes and has at its midpoint a small foramen on the ventral side. The lateral lobes border the prefrontals laterally and are superseded by the septomaxillae dorsally and anteriorly.

Nasal

In the anterior view (Fig. 3D), the ventral and medial edges of the paired nasals are straight and squared; the lateral edge is oblique, and the posterior and dorsal edges are rounded (Fig. 3C–E). The lateral edge is invaginated to form the medial wall of a large opening, which is laterally completed by the prefrontal. Similar structures are known from *Afrotyphlops punctatus* (Leach, 1819) (Cundall & Irish, 2008) and less clearly from *Rena dulcis* Baird & Girard, 1853 (Rieppel et al. 2009; weakly ossified and without clear borders) and *G. persephone* (Kraus, 2017). Remarkably, the nasal lacks the small foramina often seen in typhlopids and other scolecophidians *sensu lato* (e.g. Evans, 1955; Rieppel et al. 2009) despite the presence of numerous sensory organs on the anterior face of the head (Wallach & Ineich, 1996, our unpubl. data); the origins of the nerves that supply these organs are unclear, but possibly they arise through bundles that pass through these large openings. The medial edge of the nasals forms a medial lamina and is strongly fused to its contralateral to form the anterior component of the osseous septum nasi (terminology following Haas, 1964). At the ventromedial edge, these laminae flare to receive the anterodorsal septum of the premaxilla and brace the dorsal wall of the premaxilla. The posterior edge of the descending lamina dorsal to the premaxilla is concave, matching the profile of the septomaxilla, which follows behind it to form the posterior component of the septum nasi, completely separating the nasal cavities anterior to the vomeronasal organ. Dorsally, the extension of the lamina is the posterior-most point of the nasal. A shelf is present at the posterodorsal end of the nasal that lies beneath the frontal, which creates a large brace for that bone.

Prefrontal

The prefrontal is a more or less obtuse isosceles triangular bone in lateral view (Fig. 3A,B). Anteriorly it braces the lateral edges of the snout complex, contacting the nasals along its medial edge, premaxilla anteroventrally, frontal dorsally, and septomaxilla medially. It possesses a strong crest on its lateral face, defining the edge of the anterior plate of the skull (this crest is continued onto the frontal), and a second, lower, sigmoid crest that runs from near the dorsal end of the anterior crest to a groove located posteriorly that is continued on the lateral face of the septomaxilla (see below). Ventral to this sigmoid crest lies the maxilla, and dorsal to it is the optic region, where the heavily reduced eyes sit. Ventrally, the prefrontal forms the lateral margin of the external naris and has a small flange at its lateral edge. The posterior-most end of the prefrontal abuts but does not participate in the optical foramen in the frontal – it participates in this foramen in *A. punctatus* (Parker & Grandison, 1977), *Acutotyphlops kunuaensis* Wallach, 1995 (Cundall & Irish, 2008), and *Anilios bicolor* (Peters, 1858) (Palci et al. 2016), but in *T. jamaicensis* (Rieppel et al. 2009), *Madatyphlops* and *Indotyphlops braminus* (Daudin, 1803) (our unpubl. data) the state is as in *Xenotyphlops*. This extension of the prefrontal is somewhat spatulate and receives the lateroventral surface of the frontal in a broad, tight suture. The medial face of the bone is smooth and possesses two cup-like depressions, one just posterodorsal to the external naris, and the second at the level of the dorsolateral invagination of the nasal, in which the prefrontal participates. Most of the medial edge of the prefrontal is thickened and in contact with the septomaxilla; ventrally, just posterior to the external naris, it extends under the septomaxilla to contact the premaxilla. Posteriorly, the medial edge is sculpted to form the lateral border of the choana.

Septomaxilla

The septomaxilla is an exceedingly complicated bone (Fig. 4A–F). As in typhlopoids, it lacks a lateral flange, which is present in *Liotyphlops* (Anomalepididae; Rieppel et al. 2009). Essentially it forms the smooth-walled vomeronasal cupola around the vomeronasal organ and channels several nerves into the braincase. It is in anteroventral contact with the premaxilla, anteromedial contact with the lamina of the nasal (septum nasi), dorsomedial contact with the apex of the basisphenoid, dorsal contact with the frontal subolfactory processes, and curving lateral contact with the medial ramus of the prefrontal, and it houses but does not directly contact the vomer. Its lateral surface (Fig. 4D) forms the medial and posteromedial wall of the nostril. At its ventral end, a channel opens that transports the V_1 (trigeminal nerve) and accompanying venation from the corresponding pair of foramina in the premaxilla; the tube thereby formed is routed toward the braincase [this is essentially the same as *Liotyphlops albirostris* (Peters, 1858), Haas, 1964]. This tube has two or three small foramina along its lateral edge, i.e. along the inner wall of the nostril, and at its dorsal end, before exiting dorsally. The fate of the V_1 is not clear at this point, and will require histological sectioning or diceCT (Gignac et al. 2016) to clarify; it may enter the brain case dorsally from this exit via a fenestra formed anterior to the

subolfactory process of the frontals, but more probably it traverses the dorsal surface of the septomaxilla to enter a further channel within the ventral surface of the lateral flanges of the frontals to exit around their midpoint on the inside of the braincase, as in *Liotyphlops* (Haas, 1964). The vomeronasal organ has two dorsal foramina that enter directly into the braincase, and, if the V_1 indeed passes dorsally over this area, they must be expected to pass to one side or the other of that nerve. All of these foramina pass either side of the apex of the basisphenoid, which infiltrates into the trough of the septomaxilla at its border with the frontal. The posterior-most part of the ventral wall of the septomaxilla defines the lateral edge of the fenestra vomeronasalis, which is extended medially but not closed by the vomer. Dorsolateral to the posterior opening of the fenestra vomeronasalis there is a rounded, obliquely angled groove, which is continued on the posterior surface of the prefrontal (Fig. 3A), the function of which is unclear. The posterior wall forms the rounded lateral and dorsal edges of an opening into the roof of the mouth that is medially and ventrally weakly bounded by the vomer. The palatine lies just posterior to this opening. The posterodorsal surface of the septomaxilla forms the medial edge of the choana.

Vomer

The vomer is a delicate bone of complex topology (Fig. 5H–J). It is similar in shape to that of typhlopids (e.g. see Evans, 1955; Cundall & Irish, 2008), but its role in the nasal cupola is apparently further reduced, and it sits without osseous contact with any other bone, and does not form complete boundaries to the fenestra vomeronasalis. Posteriorly, it forms the rather rough medial and ventral edges of an opening into the roof of the mouth, bounded dorsally and laterally by the septomaxilla. It possesses a bulbous medial surface that joins it with its contralateral, a subtriangular anterior lappet that sits below but does not contact the septomaxilla, a complex lateral structure of ridges, and a long posterior ramus with a concave dorsal edge. This edge is reciprocated by the medial ramus of the palatine (see below) and is doubtless involved in its articulation. A small vomerine foramen (Oelrich, 1956) punctures this bone at the mid-point on the medial side of the fenestra vomeronasalis.

Dorsal jaw complex and palate

As in all typhlopoids, the ectopterygoid is absent (present in anomalepidids and leptotyphlopids; Cundall & Irish, 2008; McDowell, 2008), as is the postorbital (present in anomalepidids; Cundall & Irish, 2008; Rieppel et al. 2009).

Pterygoid

The elongated Y-shaped pterygoid articulates with the palatine anteriorly and is not in contact with any other bone (Fig. 5A,B). It is highly similar to that of *A. punctatus* and other typhlopoids, including *Gerrhopilus*, in general aspect (Parker & Grandison, 1977; Kraus, 2017). The anterior part is obliquely flattened, and the ventral branch of the Y formed by this flattening is much wider than the dorsal branch. The posterior bulbous flange of the palatine sits in the groove built by the branches of the Y. The pterygoid arm of the palatine follows the curve of the ventral branch of the Y. Posteriorly, the stem of the Y is long and thin, and is also obliquely compressed, rendering it elliptical in cross-section; it reaches roughly the level of the quadrate articulation with the exoccipital, around the point of the fenestra ovalis. It diverges posteriorly from its contralateral, such that it is also laterally at the level of the quadrate at its posterior extent. The posterior-most third of the elongated part of the pterygoid is slightly dorsally curved.

Palatine

The palatine is a triradiate bone, consisting of a biradial U-shaped medial component with two ventral arms, one articulating with the vomer, the other with the pterygoid, and a rod-like lateral component articulating with the maxilla (Fig. 5C–E). The vomerine arm of the U-shaped component is shorter than the pterygoid arm, curving laterally again at its distal point; this arm is separated from that of its contralateral by a narrow space that is presumably occupied by cartilage. The pterygoid arm of the U-shaped component narrows considerably toward its distal end but has a bulbous flange at its base; this shape accommodates the articulation with the anterior arms of the pterygoid. The rod-like component is thick and extends laterally beyond the lateral wall of the prefrontal at the same level, its distal end being slightly polygonal, and somewhat flattened and spatulate in posterior aspect. The lateral end pierces the palatine foramen of the maxilla, and acts as an axle on which the maxilla can rotate. This mechanism is the same as that seen in all other typhlopoids and differs strongly from those seen in Leptotyphlopidae and Anomalepididae.

Maxilla

The maxilla is a fairly simple, subtriangular bone (Fig. 5F,G). Note that because of the degree of rotation of this element, the ventral edge is posterior in the retracted state of the jaw; we here use the homologous terminology of other snakes, referring to the tooth-bearing edge as the ventral edge, and all other edges by their corresponding orientation. Its ventral edge bears four tooth loci, and it possesses four strongly recurved teeth, the largest being the first, the smallest the last. The lateral face of the bone is fairly smooth, with a large, round palatine foramen (Fig. 5F), through which the lateral component of the palatine projects (see insets of Fig. 5). The anterior and posterior edges of the bone are thickened. The anterior edge of the maxilla has a deep fossa that penetrates the bone through to the

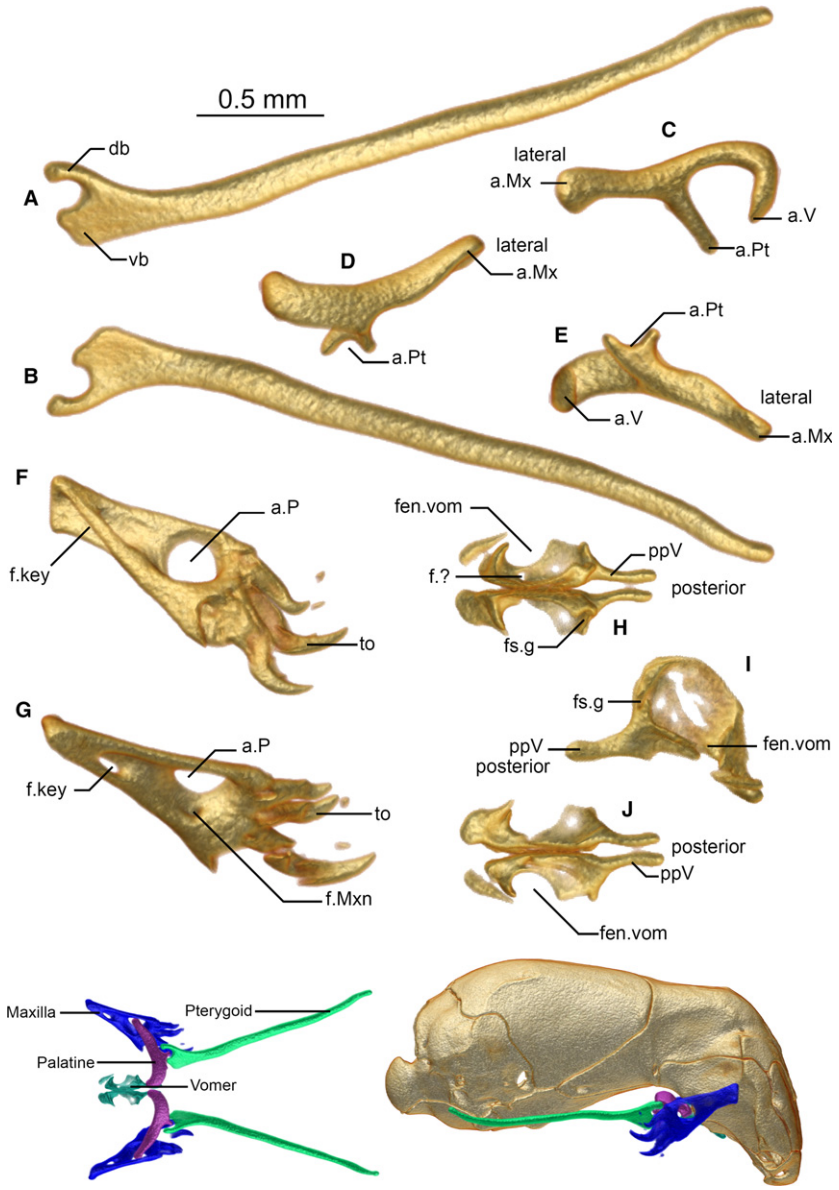

Fig. 5 Pterygoid (A,B), palatine (C–E), maxilla (F,G), and vomers (H–J) of *Xenotyphlops grandidieri* in (A,D,G,H) dorsal, (B,E,J) ventral, (C) anterior, (F) medial, and (I) lateral view. Colour insets show the articulated jaw complex in dorsal view (left) and articulated in lateral view (right). a.Mx, articulation of the palatine with the maxilla; a.P, articulation of the maxilla with the palatine; a.Pt, articulation of the palatine with the pterygoid; a.V, articulation of the palatine with the vomer; db, dorsal branch of the pterygoid; f.?, unknown foramen; f.key, keyhole foramen; f.Mxn, maxilla nerve foramen; fen.vom, fenestra vomeronasalis; fs.g, forsaken groove; ppV, posterior process of the vomer; to, tooth; vb, ventral branch of the pterygoid.

medial aspect such that a keyhole is formed (Fig. 5G). On the inner face of the maxilla, the foramen is recessed and more obvious; at the anteroventral corner of the recession, a small foramen is visible (Fig. 5G), which is probably homologous with the maxillary nerve foramen of other snakes.

The palatine foramen of the maxilla is a unique feature of typhlopoids. From a survey of the literature, we confirm its presence in *T. jamaicensis* (Evans, 1955; Rieppel et al. 2009), *Afrotyphlops blanfordii* (Boulenger, 1889), *Amerotyphlops reticulatus* (Linnaeus, 1758), *Antillotyphlops platycephalus* (Duméril & Bibron, 1844), *Indotyphlops braminus*, *Ramphotyphlops flaviventer* (Peters, 1864), *Rhinophis lineatus* (Schlegel, 1839), *Sundatyphlops polygrammicus* (Schlegel, 1839), *Typhlops pusillus* Barbour, 1914, *Typhlops rostellatus* Stejneger, 1904, *Typhlops lumbricalis* (Linnaeus, 1758), *Xerotyphlops vermicularis* (Merrem, 1820) (List, 1966), all species of *Madatyphlops* (our unpubl. data) and *G. persephone* (Kraus, 2017), but not in *Afrotyphlops*/*Megatyphlops mucroso* (Peters, 1854) (List, 1966), *A. kunuaensis* or *A. punctatus* (Cundall & Irish, 2008), or *A. bicolor* (Palci et al. 2016), where there is instead apparently a pocket on the medial face of the bone to receive the rod-like arm of the palatine (List, 1966).

Cranium

The cranium is composed of paired frontals, parietals, exoccipitals, and stapes, a basioccipital, a basisphenoid, and a small round asymmetrical element that we here tentatively refer to as a supraoccipital, but which may equally be a wormian intrasutural bone.

Frontal

The frontal is a massive bone that makes up the anterior portion of the braincase and extends at its posterior-most point beyond the midpoint of the braincase (Fig. 6A–F). The dorsal surface of the bone is flat. The frontal is posteriorly in ventrolateral contact with the basisphenoid, with this contact extending all the way forward to the septomaxilla, almost reaching the medial lamina of the nasals. It is in broad posterior contact with the parietal; this contact zone is strongly asymmetrical, as the right bone extends further posteriorly and medially than the left bone. This asymmetry is present in all three scanned specimens. The frontal forms the subolfactory process by the medial contact of its lateral flanges posterior to the septomaxilla and over the apex of the basisphenoid. A broad, medial foramen is present anterior to the subolfactory process, and presumably receives the vomeronasal nerves from the septomaxilla below. Along the lateral walls of this foramen, the frontal is in contact with the dorsal facet of the septomaxilla. Anteriorly, it is in ventrolateral contact with the prefrontal, and anteriorly and anteromedially it is in ventral contact with the nasal and the dorsal extent of the medial lamina of the nasal. Through these relationships, it forms the dorsal component of the anterior wall of the skull. The lateral surface of this anterior extent of the frontal possesses a ridge that continues the lateral ridge of the prefrontals in defining the anterior wall of the skull (Fig. 6B,C,F). A further ridge is present at the posterior extent of the prefrontal (Fig. 6C), running vertically from this position to the parietal. At the anteromedial-most point of the bone, the frontal extends downwards and overlaps the nasal strongly, a relationship seen also in typhlopids and presumably also gerrhopilids (not clear from Kraus, 2017) but without the downward inflection, and differing strongly from the states seen in Leptotyphlopidae and Anomalepididae (Rieppel et al. 2009). The resulting lappet has a weak medial groove (Fig. 6B), and does not follow the septum perfectly, instead forming an unusual invagination of unknown function between it and its contralateral. The ventral side of the bone has a hollowed area that anteriorly houses the olfactory complex and routes the nostril to the choana. The subolfactory process forms the posterior border of the choana. Posterior to this, it possesses a large facet for the junction of the prefrontal, posterior to which it is free.

The inside of the frontal is rather smooth, without acute ridges. Numerous large foramina are present on the interior frontal: one at the posterior-most corner of the bone (probably transporting the maxillary ramus of the trigeminal nerve, V_2); two at its midpoint, one exiting laterally (presumably containing the optic nerve), and one exiting anteromedially at the posterior edge of the contact with the septomaxilla (presumably channelling V_1); a broad medial foramen between the subolfactory processes at the level of the septomaxilla that presumably channels all the nerves of the vomeronasal organ; a large opening just posterior to the nasal contact, apparently opening into the nostril cavity (function unknown; we know of no comparable features in other snakes, but this should be searched for in other taxa); and a small foramen at the dorsal end of the prefrontal-frontal vertical ridge.

Basisphenoid

The basisphenoid is a long, triangular bone that runs from the basioccipital posteriorly to invade the septomaxilla anteriorly, almost reaching the medial lamina of the nasal (Fig. 7D–F). It is in extensive dorsolateral contact with the frontal, brief lateral contact with the parietal, posterolateral contact with the exoccipitals, and posterior contact with the basioccipital. The ventral surface of the bone (Fig. 7F) is more or less smooth, with a single medial depression at the level of the posterior-most extension of the prefrontal, and two ventrolateral basisphenoid apophyses toward the posterior end of the bone, which continue as ridges onto the anterolateral ventral surface of the basioccipital (Fig. 7C). A comparable feature is not visible from other typhlopoids thus far examined by us (largely *Madatyphlops* spp., our unpubl. data, but see also *T. jamaicensis* in Rieppel et al. 2009 and *G. persephone* in Kraus, 2017). The dorsal surface of the bone (Fig. 7D) is as smooth as the inside of the frontal, possessing a single pair of small foramina that run from the inside of the bone posterolaterally out of the skull, along a corresponding groove in the exoccipital, which carry the carotid artery (McDowell, 2008). This groove is called the vidian canal by Rieppel et al. (2009) and vidian groove by Cundall & Irish (2008).

Parietal

The parietal is paired (Fig. 7G,H). It is a large bone that continues the shape of the frontal anteriorly. It is in contact with the frontal anteriorly and anteroventrally, with the exoccipital and the supraoccipital (see below) posteriorly, and it has a brief contact zone with the basisphenoid ventrally. The dorsal face is nearly flat, the posterior part of the bone being curved ventrally. The lateral surface (Fig. 7G) is slightly curved; it is separated from the dorsal surface by a ridge which is accentuated at its posterior end. Anteriorly, this ridge is barely recognisable as it is very low, and a small tuberosity is present at the angle where the anterior edge of the parietal turns posteroventrally. This tuberosity is a widespread feature within the Typhlopidae, where it can be extremely strongly accentuated (e.g. *T. jamaicensis* in Rieppel et al. 2009 and *A. punctatus* in Haas, 1930). It is absent in *G. persephone* (Kraus, 2017). The parietal shows no openings. The inner surface (Fig. 7H) is smooth and rounded. The posterior edge is straight; only the right parietal bone has a small dorsomedial groove giving way to the small supraoccipital (see below). The posterolateral contact

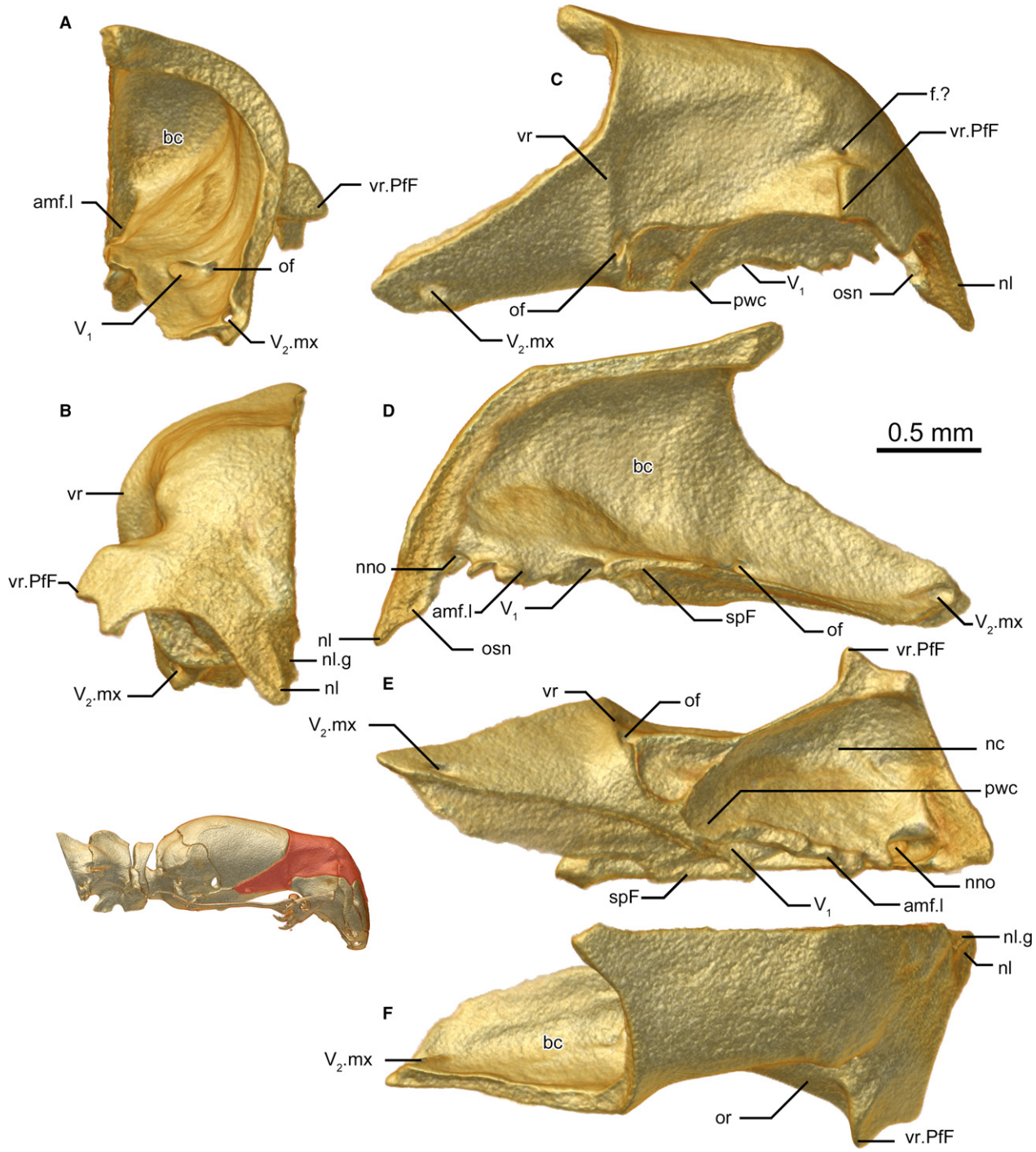

Fig. 6 Frontal of *Xenotyphlops grandidieri* in (A) posterior, (B) anterior, (C) lateral, (D) medial, (E) ventral, and (F) dorsal view. amf.l, lateral wall of anterior medial foramen; bc, braincase; f.?, unknown foramen; nc, nasal cavity, nostril; nl, nasal lappet; nl.g, nasal lappet groove; nno, nostril nerve opening; of, optic foramen; or, optic recession; osn, osseous septum nasi; pwc, posterior wall of the choana; spF, subolfactory process of the frontal; V_1, trigeminal; V_2.mx, maxillary (V_2) branch of the trigeminal; vr, vertical ridge; vr.PfF, prefrontal-frontal vertical ridge.

zone with the exoccipital is wavy, and at its lateral margin overlaps a portion of that bone (Fig. 7H).

Pairing of the parietals is variable in Anomalepididae, Leptotyphlopidae, and Typhlopoidea (Cundall & Irish, 2008; Kraus, 2017).

Supraoccipital

There is a small asymmetrical element located between the parietals and the exoccipitals, sitting to the right of the midline (Figs 2D and 7). The position and relationships of this bone argue for it to be termed the 'supraoccipital', but

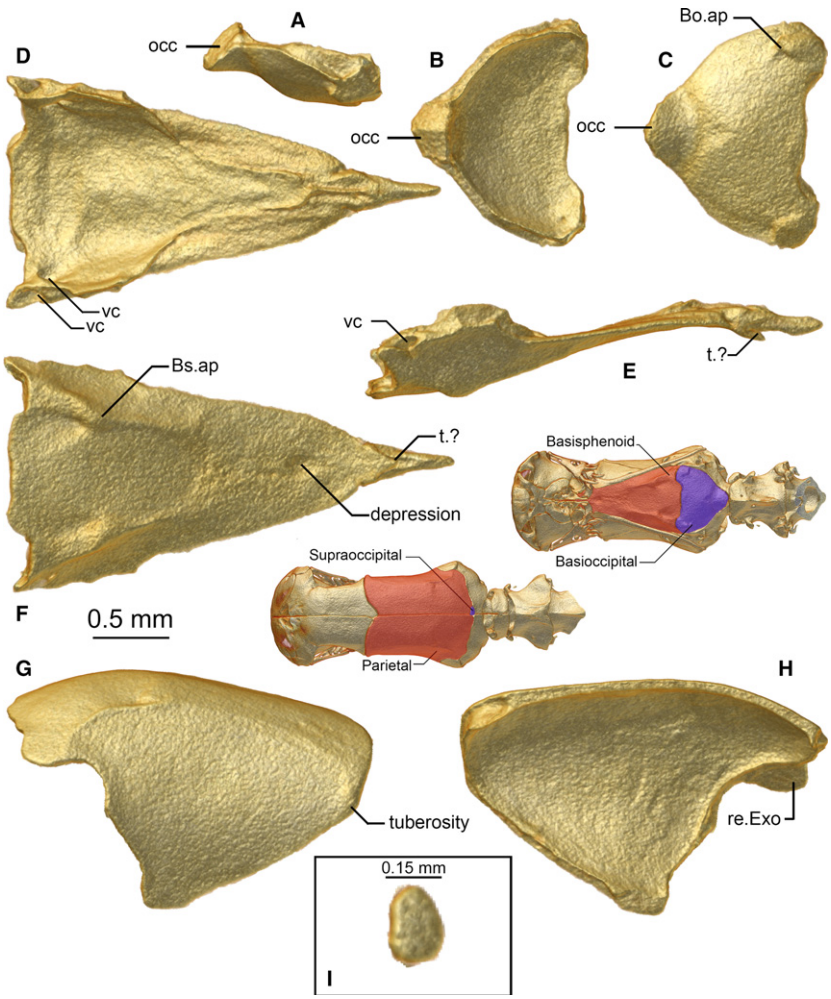

Fig. 7 Basioccipital (A–C), basisphenoid (D–F), parietal (G,H), and supraoccipital (I) of *Xenotyphlops grandidieri* in (A,E,G) lateral, (H) medial, (B,D,I) dorsal, and (C,F) ventral view. Bo.ap, basioccipital apophysis; Bs.ap, basisphenoid apophysis; occ, occipital condyle; re.Exo, receiving surface for the exoccipital; t.?, tubercle of unknown function; vc, vidian canal.

homology with that element in other snakes has yet to be established. It is only present in the segmented specimen; in both ZSM 2216/2007 and ZSM 2213/2007 its place is occupied by the parietals. If it is homologous with the supraoccipital, then it may be an atavism or idiosyncrasy present in only some individuals of the species. Alternatively, as mentioned above, it may be a wormian intrasutural bone, and therefore simply an anomaly.

Basioccipital

The basioccipital is a thick, subtriangular bone which is in contact with the basisphenoid anteriorly and the exoccipital posteriorly to laterally (Fig. 7A–C). The anterior edge of the bone is medially straight and shows rectangular elongations on the sides, where the bone is thickened to continue the ridge of the basisphenoid apophyses and forms basioccipital apophyses (termed basioccipital tubercles by Palci et al. 2016). The basioccipital has a slightly curved contact zone with the exoccipital laterally, and the posterior apex is ventrally expanded so that the posteriormost contact between the basioccipital and the exoccipital is strongly thickened, to brace and possibly participate in the occipital condyle, as in other scolecophidians *sensu lato* (Cundall & Irish, 2008).

Exoccipital + Prootic

The exoccipital and prootic are fused to form a single, robust element that is a curved, cuplike bone that braces the posterolateral corners of the skull (Fig. 8A–F). Its lateral wall houses the otic complex, which is remarkably well developed and contains almost entirely within it the stapes (see below). The quadrate lies just exterior to this portion of the bone, and its medial face closely matches the shape of the external face of the exoccipital. The exoccipital is in broad anterior contact with the parietal, brief anteroventral contact with the basisphenoid, broad ventral contact with the basioccipital, and brief contact with the small supraoccipital, and posteriorly articulates with the atlas–axis complex (seemingly fused elements). The pathways of the semicircular canals are not obvious externally, and we did not examine their internal shape in detail. The outer face of the exoccipital (Fig. 8A–C,E) possesses several ridges, most distinctly one sigmoid ridge from the anterolateral corner, which continues that seen externally on the posterolateral

parietal, descending halfway down the otic corpuscle before running horizontally posteromedially toward, but not participating in, the foramen magnum. The foramen magnum is an exclusively exoccipital opening, and its dorsal lip extends slightly laterally and ends in a bulbous projection perpendicular to the aforementioned ridge arising from the parietal, but not reaching it. At its posteroventrolateral corner, the bone possesses a channel that leads to the posterior foramen of the basisphenoid, which routes the carotid artery. At the anterior edge of this channel is a small foramen entering into the trigeminal foramen (see below).

Five foramina are present on the outside of the exoccipital: an anterolateral foramen that enters the braincase (trigeminal foramen, $V_2 + V_3$), a posterolateral opening near the level of the posterior extent of the quadrate (the fenestra ovalis, see below); a ventrally oriented foramen just behind and below the fenestra ovalis (the recessus scalae tympani, housing the foramen of the vagus nerve); two foramina, one dorsal and one ventral to the bulbous process at the lateral edge of the lip of foramen magnum (the ventral being the vagus nerve foramen, the dorsal of unknown function); and one foramen in the dorsal edge of the posterior articulatory extension that also joins the ventral of this pair of foramina (presumably a further vagus nerve foramen).

The inner surface of the exoccipital possesses at least 10 foramina. The largest of these is anterior and corresponds to the trigeminal foramen, which forms a depression in the wall of the exoccipital anterior to the otic capsule; two small foramina open into this depression, one ventrally (that which connects to the anterior edge of the carotid channel, mentioned above) and one posteriorly. Next to this depression a pair of small foramina is present at roughly the mid-level of the otic capsule, corresponding to the acoustic nerve foramina. The second-largest foramen is posterior to the otic capsule (vagus foramen), and beside it a further small foramen exists (function unknown). A pair of unevenly sized foramina is present on the ventral posteromedial wall of the otic capsule, just anterior to the vagus foramen; the anterior of these is the perilymphatic foramen, and the posterior is the recessus scalae tympani medial aperture (Rieppel et al. 2009). A small, dorsally oriented foramen corresponding to the endolymphatic foramen is present in the dorsal portion of the otic corpuscle. Finally a small foramen sits below the dorsal arch of the exoccipitals that exits posteriorly and another is present on the inner surface of the occipital condyle (functions unknown). The posterior articulatory surface of the occipital condyle is typical of typhlopoids, with a ball-like extension.

Stapes

The stapes is similar to that of typhlopids but has an exceptionally short stylus. It sits almost wholly recessed within the fenestra ovalis of the exoccipital (Fig. 8B,C,E).

Suspensorium

The mandible of *Xenotyphlops* is highly similar to that of typhlopoids and differs only in its more bent profile and finer details of the structures of some of the bones (Figs 9 and 10).

Quadrate

In lateral view (Fig. 9E) the quadrate is a laminar, slightly convex, triangular bone, composed of three processes: the otic process (posterior), the cephalic process (anterodorsal), and the mandibular process (anteroventral). It is flattened from the midpoint posteriorly, but at its thinnest at the midpoint (Fig. 9E,F). Anteriorly it grows thicker and rounder until the rounded apex of the mandibular process, which articulates with the compound. The posterior apex of the otic process presumably articulates via a cartilaginous link with the stapes, and has a rounded shape in lateral view; a weakly raised vertical ridge is present on the lateral face at the level of the fenestra ovalis. This is probably the attachment point for the caudal-most mandibular adductor muscle, common among typhlopids (Haas, 1930, 1973). The shape of the bone differs from gerrhopilids in having its cephalic process more posteriorly situated on the bone (Kraus, 2017). It differs from typhlopids, in having its cephalic process more posteriorly situated on the bone, and being less acute and shorter. A small foramen is present on the lateral face slightly anterior to the midpoint of the quadrate. This foramen is more developed on the right bone in ZSM 2194/2007. The two other specimens show a second small foramen on the lateral face of the quadrate, situated further posteriorly. However, it is only present on the right quadrates of these specimens (see Variation section below).

Compound

The compound bone has a bent profile in lateral view (Fig. 9C), possessing an elongated, thin, horizontally flattened retroarticular process, a clear, broad articular facet for the articulation with the quadrate, and a deep mandibular fossa at the level of the ventral curve of the bone (Fig. 9A–D). In structure and relationships, it is very like the compound of typhlopoids, but much more strongly bent downwards. It houses the Meckelian canal, which runs from the mandibular fossa forward, exits along the internal face of the bone behind the coronoid (Fig. 9D), and extends toward the dentary. The compound is in broad medial contact with the coronoid, in ventral contact with the angular, and brief anterior contact with the splenial, where it approaches but does not contact the dentary. It bears two foramina along its anterior lateral surface (anterior and posterior surangular foramina), and one at the level of the

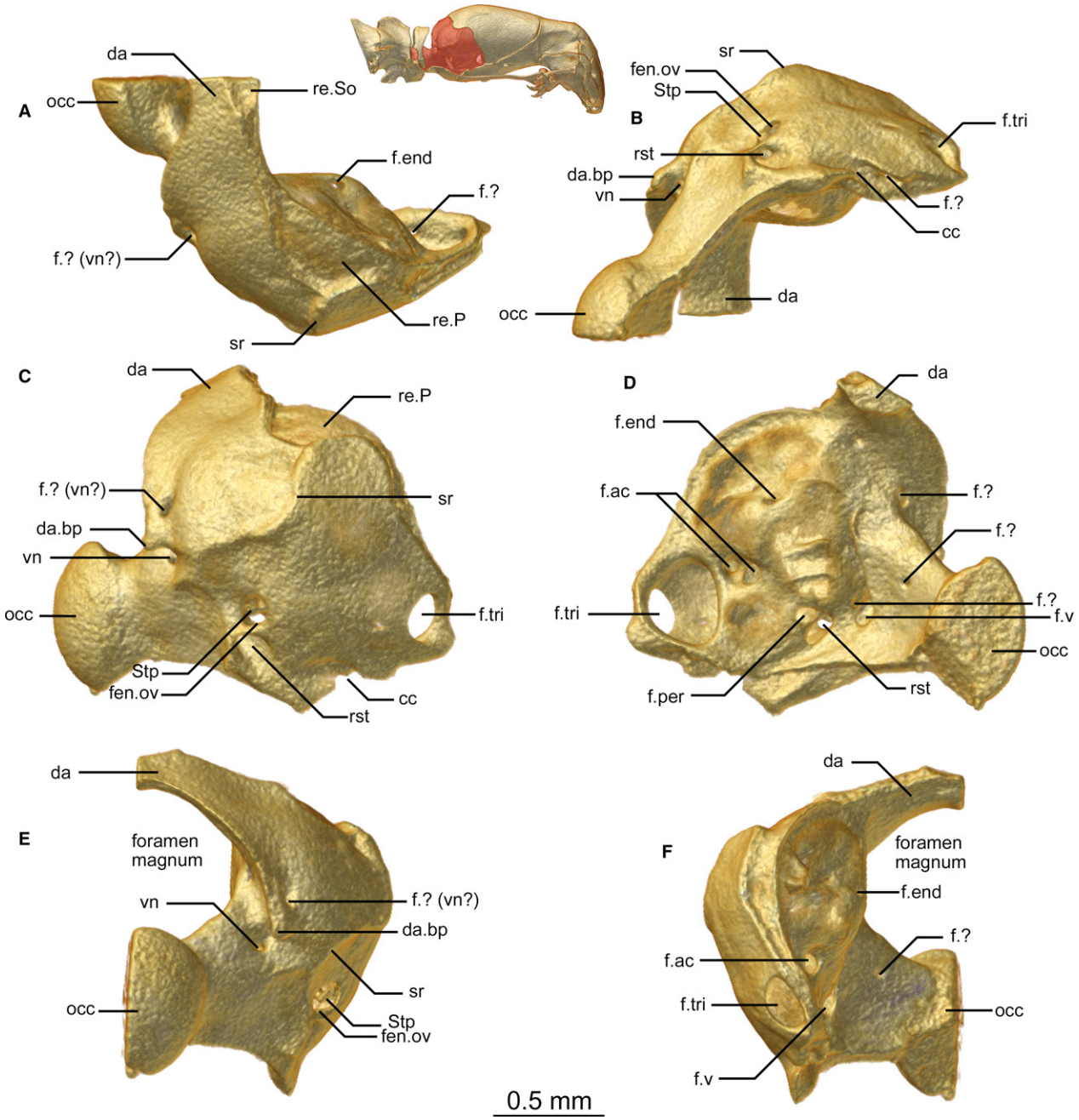

Fig. 8 Exoccipital of *Xenotyphlops grandidieri* in (A) dorsal, (B) ventral, (C) lateral, (D) medial, (E) posterior, and (F) anterior view. cc, carotid channel; da, dorsal arch of the exoccipital; da.bp, bulbous process at base of the dorsal arch of the exoccipital; f.?, unknown foramen; f.ac, acoustic foramen; f.end, endolymphatic foramen; f.per, perilymphatic foramen; f.tri, trigeminal foramen; f.v, vagus foramen; fen.ov, fenestra ovalis; occ, occipital condyle; re.P, receiving surface for the parietal; re.So, receiving surface for the supraoccipital; rst, recessus scalae tympani; sr, sigmoid ridge; Stp, stapes; vn, vagus nerve.

articulation with the quadrate (for the chorda tympani nerve, CN7).

Coronoid

The coronoid is a curved laminar bone with a triangular general shape in lateral view (Fig. 10G,H). It sits on the inner side of the compound, the posterodorsal apex fitting in the cavity of the compound. The anterodorsal apex is acuminate and elongated. The ventral apex, which is as long and as acuminate as the anterodorsal one, reaches towards the posterior cavity of the dentary and is ventrally bound with the splenial. The shape and relationships of this bone strongly resemble those of other typhlopoids (Cundall & Irish, 2008; Kraus, 2017), and differs considerably from

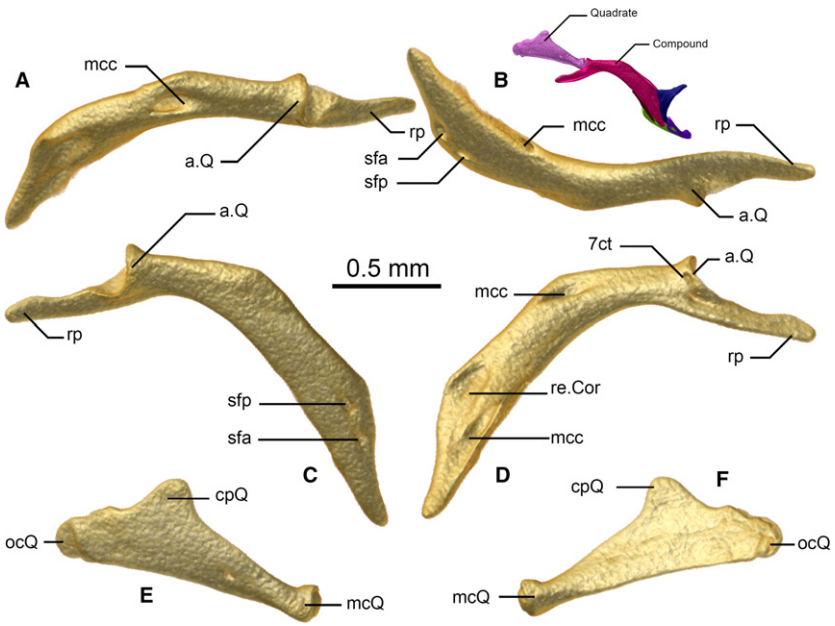

Fig. 9 Compound (A–D) and quadrate (E,F) of *Xenotyphlops grandidieri* in (A) dorsal, (B) ventral, (C,E) lateral, and (D,F) medial view. Coloured inset is the right jaw in lateral view. 7ct, chorda tympani nerve, CN7; a.Q, articulation of the compound with the quadrate; cpQ, cephalic process of the quadrate; mcc, Meckelian canal; mcQ, mandibular process of the quadrate; ocQ, otic process of the quadrate; re.cor, receiving surface for the coronoid; rp, retroarticular process; sfa, anterior surangular foramen; sfp, posterior surangular foramen.

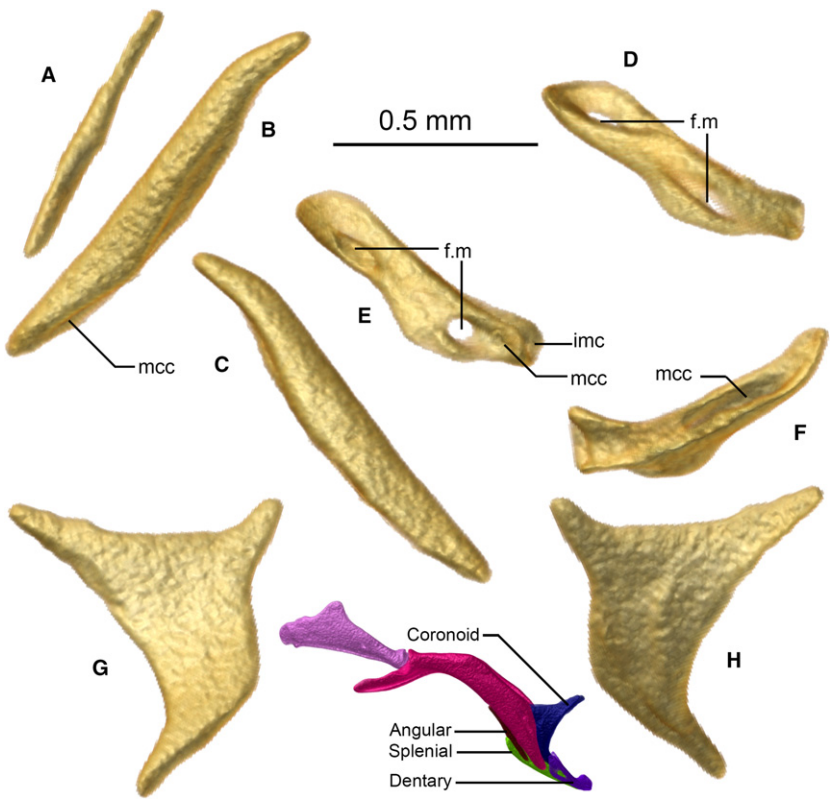

Fig. 10 Angular (A), splenial (B,C), dentary (D–F), and coronoid (G,H) of *Xenotyphlops grandidieri* in (B,D) dorsal, (C,E) ventral, (F) posterior, (A,G) medial, and (H) lateral view. Colour inset is the right jaw in lateral view. f.m, mental foramen; imc, intermandibular cartilage; mcc, Meckelian canal.

that seen in leptotyphlopids, where it is a small bone situated dorsal to the compound, and anomalepidids, where it is a broad, flared bone with a curved anterior edge (Cundall & Irish, 2008; Rieppel et al. 2009).

Angular

The angular is a simple, thin bone that lies against the posterior surface of the anterior end of the compound, and anteriorly is in lateral contact with the splenium (Fig. 10A). It briefly underlies the Meckelian canal before the ventral extension of the coronoid encloses it.

Splenial

The splenial is a simple, rather straight bone that is thicker and considerably longer than the angular (Fig. 10B,C). It runs from the middle of the angular forward and downward toward the end of the mandible at the apex of the dentary, and is in contact with the compound and angular posteriorly, coronoid posterodorsally, and dentary anteriorly and laterally. Its dorsolateral surface is slightly curved to guide the Meckelian canal, and it forms the posteroventral wall of the canal for its length along the dentary.

Dentary

The dentary is a rather hollow, tube-like bone that is slightly flattened at its midpoint, and slightly ventrally bowed (Fig. 10D–F). It is in posterior contact with the splenial, houses the ventral apex of the coronoid in the medial cavity of its posterior edge, and posteriorly it approaches but does not contact the compound. As in all other typhlopoids, it is edentulous. It bears two large foramina on its anterior edge, one at either end, and posteriorly is grooved for the Meckelian canal. The medial end of the dentary is somewhat dorsoventrally flattened, and on one side has an oblong dorsal foramen; its distal surface is flattened to house the medial intermandibular cartilage (Bellairs & Kamal, 1981).

Variation

The following variation was observed among the skulls of the three micro-CT scanned specimens examined here (for reference, see Figs S1–S3 of the three specimens):

As noted above, only ZSM 2194/2007 has a 'supraoccipital' bone. In the two other specimens, this bone is totally absent, its place being taken by the parietals.

The foramina transporting the ophthalmicus profundus (V_1) nerve on the ventral side of the premaxilla are asymmetrical in ZSM 2194/2007 (the left ones not being separated) but separated on both sides in the two other specimens. This is almost certainly a growth defect of ZSM 2194/2007. All other scolecophidians have four distinct foramina, too (Rieppel et al. 2009).

The opening between the nasal and prefrontal is entirely circled by the nasal in ZSM 2216/2007. In the two other specimens, its lateral wall is formed by the prefrontal. Similar variation was also noted in the trigeminal foramen at the anterolateral edge of the exoccipital. It lies entirely within the exoccipital in ZSM 2194/2007 and ZSM 2213/2007, although the parietal very closely abuts its lateral wall. In ZSM 2216/2007 the parietal forms the complete anterior wall of this foramen.

In ZSM 2216/2007, the lateral horizontal groove dorsally to the prefrontal-frontal ridge (defining the anterior plate of the skull) is slightly deeper than in the other specimens.

The medial contact zone between the basisphenoid and the basioccipital is straight in ZSM 2194/2007, posteriorly rounded in ZSM 2213/2007, and irregular and asymmetrical in ZSM 2216/2007, although it is more similar to the curved shape than to the straight.

The quadrate shows variability in two aspects: its cephalic process is less acute in ZSM 2213/2007 than in the other specimens, and the foramina on its lateral side are differently developed. ZSM 2194/2007 shows only the anterior foramen, the one on the left bone being very small. ZSM 2216/2007 shows a strong asymmetry between its two quadrates: the right one bears both the anterior and posterior foramina, and on the left bone they are nearly absent (only recognisable when one knows where to search for them). ZSM 2213/2007 has the two foramina on the right side, but only the anterior one on the left side.

The anteroventral-most foramina of the dentary show similar variation. ZSM 2194/2007 displays one broad foramen on each side. ZSM 2216/2007 has one broad foramen on the right side and two smaller ones, close to each other but separated, on the left side. ZSM 2213/2007 has two separated small foramina on the right side and a broad one on the left side.

Discussion

Why so weird?

The skull of *X. grandidieri* is unique among scolecophidians in a number of aspects. Some of these, such as the unusual shape of the quadrate with its displaced and shortened cephalic process and presence of basisphenoid tubercles and ridges, are rather minor details, and on the whole, it resembles the skulls of Typhlopidae and Gerrhopilidae. However, the ventral inflection of the snout is a major difference to other scolecophidians *sensu lato*. This inflection results in several rearrangements in the relationships between bones compared with other typhlopoids. It results in the characteristic anterior shield of the head, which possesses numerous sensillae; these were important features in the recognition of *Xenotyphlops* as its own genus (Wallach & Ineich, 1996). As a consequence of the skull inflection, the lower jaw is also considerably bent in comparison with other typhlopoids, and the mouth opening is more ventrally oriented.

At present, a functional or adaptive underpinning of the unusual shape of the *Xenotyphlops* skull remains unknown. Here we put forward four potential explanations for the evolution of the unusual skull shape of this snake:

1 Phragmosis. The robust, round, rather flat and smooth head shield of the snake may be used to block its burrows from potential predators or competitors, in a method similar to that seen in insects, anurans, and mammals (Macalister, 1875; Wheeler, 1927; Jared et al. 2005), with corresponding morphological adaptations.
2 Sensory perception. *Xenotyphlops* are characterised by a high density of long sensillae on their anterior head plate (Wallach & Ineich, 1996). Similar, possibly homologous structures have also been reported from *Letheobia* cf. *caeca* (Young & Wallach, 1998), and indeed from several other typhlopids (Haas, 1932; Gabe & Saint Girons, 1967), although these are generally much shorter (Young & Wallach, 1998). Young & Wallach (1998) suggested that the sensillae function as mechanoreceptors, with a tactile role. We posit that they could additionally function to detect vibrations in the burrowing substrate, and thus aid in the detection of prey and predators over larger distances. Downward inflection of the rostrum may have provided a greater anterior surface of the head for the placement of sensillae. Possibly this regionalisation of the sensillae anteriorly may provide increased directionality of sensitivity for *Xenotyphlops.*
3 Feeding protection. Although the composition of the diet of *Xenotyphlops* is not yet known, it is likely that it feeds on ants or termites, as is common to all scolecophidians. A more ventral opening of the mouth may permit the snake to feed on larvae or eggs from above, while warding off defensive attacks from guards (e.g. ant soldiers) through its rostral shield and the scales of its head.
4 Adaptation to sandy substrate. *Xenotyphlops* occurs exclusively in coastal, loose sandy substrates. Inflection of the mouth downwards results in the ventral position of the external nares and the mouth. This repositioning may reduce the amount of sand and dust that enters the orifices.

Ultimately, it is likely that the adaptive value of the inflection of the rostrum is a combination of these and other factors, and more detailed analysis of the ecology of the species is required before conclusions can be drawn.

Xenotyphlopidae in relation to Typhlopoidea and Scolecophidia *sensu lato*

In addition to the remarkable inflection of the skull, the following characters were noted to differ significantly in their shape and/or relationships from the typical typhlopid skull, and that of *G. persephone* (which is highly similar to a typical typhlopid skull):

The shape of the quadrate differs considerably from other typhlopoids, in having a shorter and more acute overall profile, and a more posteriorly shifted cephalic process. The septomaxilla is largely excluded, and the nasal wholly excluded, from participation in the naris; both of these bones typically participate in the naris in typhlopoids (Cundall & Irish, 2008; Rieppel et al. 2009). Finally, the presence of basisphenoid apophyses is not known from other typhlopoids, to our knowledge.

The skull of *Xenotyphlops* is exceptionally robust and the bones very strongly fused. As a result, we suspect that its skull is largely akinetic, except for the purpose-built jaws. This is apparently somewhat different from other typhlopids, some of which have meso- and possibly prokinetic joints between the frontals and parietals (Cundall & Irish, 2008; Evans, 2008; Kraus, 2017). However, more extensive studies of skull kinesis in typhlopoid snakes are needed.

Despite its uniqueness, the skull of *Xenotyphlops* shares numerous characters with typhlopid and gerrhopilid species that are synapomorphic to this clade. These features include: (1) maxilla-palatine-pterygoid-vomer configuration into a rotational jaw used in 'maxillary raking' (Kley, 2001), (2) an edentate dentary, (3) the absence of a postorbital and ectopterygoid, (4) paired nasals, (5) absence of lateral flange of septomaxilla, (6) frontal anteriorly overlapping the nasal, and (7) an acute and triangular coronoid process. Of these features, the jaw mechanism is the most distinctive feature among the typhlopoids. As we discuss below, the typhlopoid mechanism is wholly different from Leptotyphlopidae and Anomalepididae, but we posit that the three separate jaw structures converged at a functional level in response to a specialisation in each of the three (super)families for a diet consisting of eusocial insects.

Miniaturisation and rearrangement of eusocial-insect-gobbling jaws

It has long been discussed that scolecophidians may be surviving representatives of the primitive state of snakes (Bellairs & Underwood, 1951; Miralles et al. 2018). For almost the same duration of time, others have argued that scolecophidians represent rather independent specialisation for burrowing habits, deviating significantly from the trends of snake evolution (Evans, 1955), and are rather more derived than ancestral. Most scolecophidians *sensu lato* are small or very small, and include the world's smallest snakes (Hedges, 2008). Miniaturisation has a well-known role in causing rearrangement and homoplasy of bauplans (Hanken & Wake, 1993). Even when the overall bauplan is maintained, miniaturisation can lead to the emergence of novel developmental and morphological relationships (Hanken & Wake, 1993; Clarke, 1996).

Ecologically, typhlopoids, leptotyphlopids, and anomalepidids are highly similar: they are all fossorial, generally small (sometimes extremely miniaturised) snakes, most of whose diet consists largely, if not exclusively, of eusocial insects (Webb & Shine, 1993; Kley, 2001, 2006; Webb et al. 2001). Although there is a list of osteological characters that appear to unite these clades, their jaw morphology led Cundall & Irish (2008) to suggest that they are a paraphyletic group. Indeed, the arrangement of key bones involved in the upper and lower jaws differ strongly among the separate clades.

In Leptotyphlopidae, the prefrontal is integrated in the snout complex, the maxilla is edentate and sits on the prefrontal, and is presumably fixed in position. The pterygoids are thin and palatines broad, and all appear to be similarly fixed. The mandible is robust and contains an intramandibular joint between the angular and splenial involved in mandibular raking (Kley, 2006), and the dentary bears teeth.

In Anomalepididae, the prefrontal and maxilla have both been occluded from the snout complex; the prefrontal articulates with the frontal posteriorly and maxilla anteriorly; the maxilla bears teeth and articulates with the prefrontal dorsally/proximally, and with the ectopterygoid (absent in all other scolecophidians *sensu lato*) ventrally/distally, which in turn articulates posteriorly with the pterygoid; the pterygoid is braced anteromedially by the palatine (Cundall & Irish, 2008; Rieppel et al. 2009). The mandible is slender and edentulous.

In Typhlopoidea, the prefrontal is integrated in the snout complex, the maxilla bears teeth, and is occluded from the snout complex, and articulates on an axle-like extension of the palatine, which together with the pterygoid is presumably involved in the maxillary raking mechanism (Kley, 2001). The mandible is slender and edentulous.

Current molecular phylogenetic evidence suggests that Scolecophidia are not monophyletic, with the Leptotyphlopidae and Typhlopoidea forming a clade (Scolecophidia *stricto sensu* in Miralles et al. 2018), and the Anomalepididae being more closely related to Alethinophidia (Fig. 1). All three groups differ strongly in jaw morphology, with the Typhlopoidea using maxillary raking, Leptotyphlopidae using mandibular raking, and the Anomalepididae using maxillary raking with a different jaw configuration from Typhlopoidea. Indeed, the jaws themselves do not seem to present arguments favouring any particular phylogenetic relationships among the scolecophidian clades; any arrangement requires dramatic reshuffling of several bone elements. This situation is doubtless a reflection of the ancient branching between the scolecophidian clades (Vidal et al. 2010; Miralles et al. 2018). We suggest that the dramatic differences in morphology, but similar functional outcomes of the feeding mechanisms of scolecophidians *sensu lato*, are a result of miniaturisation and convergent evolution, as opposed to being representative of the ancestral snake ecomorphology. If the miniaturisation that we hypothesise gave rise to each jaw arrangement, their evolution was convergent and independent at the base of each of these three major lineages, which would explain why the jaws within each group have not subsequently diversified strongly.

To test this hypothesis, we need robust phylogenomic trees to establish how stable the relationships of the Scolecophidia *sensu lato* are, and the osteology of vertebral column for a wider selection of these snakes. Soft tissue analysis by diceCT (Gignac et al. 2016) may also provide an array of new data for constructing morphological phylogenies, while also enabling us to study in greater detail the internal anatomy of these unusual snakes. Of particular interest will be the olfactory bulb and understanding the enervation of the anterior plate and its sensillae.

Acknowledgements

We wish to thank Alex Cerwenka and Bernhard Ruthensteiner for facilitation of micro-CT scans.

Conflict of interest

We know of no conflicts of interest.

Author contributions

J.C. and M.D.S. contributed to the conception of the study, gathering of data, data analysis, and drafting and critical revision of the article. C.Y.W.-C. helped in data interpretation and critical revision of the article. F.G. contributed to the conception of the study and critical revision of the article.

References

Bellairs AdA, Kamal AM (1981) The chondrocranium and the development of the skull in recent reptiles. In: *Biology of the Reptilia*. (eds Gans C, Parsons TS), pp. 1–263. London: Academic Press.

Bellairs AdA, Underwood G (1951) The origin of snakes. *Biol Rev Camb Philos Soc* **26**, 193–237.

Burbrink FT, Crother BI (2011) Evolution and taxonomy of snakes. In: *Reproductive Biology and Phylogeny of Snakes*. (eds Aldridge RD, Sever DM), Chapter 2, pp. 19–53. Boca Raton: CRC Press.

Clarke BT (1996) Small size in amphibians – its ecological and evolutionary implications. *Symp Zool Soc London* **69**, 201–224.

Cundall D, Irish FJ (2008) The snake skull. In: *The Skull of Lepidosauria*. (eds Gans C, Gaunt AS, Adler K), pp. 349–692. Ithaca, NY: Society for the Study of Amphibians and Reptiles.

Cundall D, Wallach V, Rossman DA (1993) The systematic relationships of the snake genus *Anomochilus*. *Zool J Linn Soc* **109**, 275–299.

Evans HE (1955) The osteology of a worm snake, *Typhlops jamaicensis* (Shaw). *Anat Rec* **122**, 381–396.

Evans SE (2008) The skull of lizards and Tuatara. In: *The Skull of Lepidosauria*. (eds Gans C Gaunt AS, Adler K), pp. 1–348. Ithaca, NY: Society for the Study of Amphibians and Reptiles.

Figueroa A, McKelvy AD, Grismer LL, et al. (2016) A species-level phylogeny of extant snakes with description of a new colubrid subfamily and genus. *PLoS One* **11**, e0161070.

Forstner MRJ, Davis SK, Arévalo E (1995) Support for the hypothesis of anguimorph ancestry for the suborder Serpentes from phylogenetic analysis of mitochondrial DNA sequences. *Mol Phylogenet Evol* **4**, 93–102.

Gabe M, Saint Girons H (1967) Données histologiques sur le tégument et les glandes épidermoïdes céphaliques des Lépidosauriens. *Acta Anat* **67**, 571–594.

Gignac PM, Kley NJ, Clarke JA, et al. (2016) Diffusible iodine-based contrast-enhanced computed tomography (diceCT): an emerging tool for rapid, high-resolution, 3-D imaging of metazoan soft tissues. *J Anat* **228**, 889–909.

Haas G (1930) Über das Kopfskelett und die Kaumuskulatur der Typhlopiden und Glauconiiden. *Zool Jahrb Abt Anat* **52**, 1–94.

Haas G (1932) Über drüsenähnliche Gebilde der Epidermis am Kopfe von *Typhlops braminus*. *Z Zellforsch Mikrosk Anat* **16B**, 745–752.

Haas G (1959) Bemerkungen über die Anatomie des Kopfes und des Schädels der Leptotyphlopidae (Ophidia), speziell von *L. macrorhynchus* Jan. *Vierteljahrsschr Naturforsch Ges Zürich* **1959**, 90–104.

Haas G (1964) Anatomical observaitons on the head of *Liotyphlops albirostris* (Typhlopidae, Ophidia). *Acta Zool* **45**, 1–62.

Haas G (1973) Muscles of the jaws and associated structures in the Rhynchocephalia and Squamata. In: *Biology of the Reptilia*. (eds Gans C, Parsons TS), pp. 285–490. London: Academic Press.

Hanken J, Wake DB (1993) Miniaturization of body size: organismal consequences and evolutionary significance. *Annu Rev Ecol Syst* **24**, 501–519.

Harrington SM, Reeder TW (2017) Phylogenetic inference and divergence dating of snakes using molecules, morphology and fossils: new insights into convergent evolution of feeding morphology and limb reduction. *Biol J Linn Soc* **121**, 379–394.

Hedges SB (2008) At the lower size limit in snakes: two new species of threadsnakes (Squamata: Leptotyphlopidae: *Leptotyphlops*) from the Lesser Antilles. *Zootaxa* **1841**, 1–30.

Heise PJ, Maxson LR, Dowling HG, et al. (1995) Higher-level snake phylogeny inferred from mitochondrial DNA sequences of 12S rRNA and 16S rRNA genes. *Mol Biol Evol* **12**, 259–265.

Hsiang AY, Field DJ, Webster TH, et al. (2015) The origin of snakes: revealing the ecology, behavior, and evolutionary history of early snakes using genomics, phenomics, and the fossil record. *BMC Evol Biol* **15**, 87.

Jared C, Antoniazzi MM, Navas CA, et al. (2005) Head co-ossification, phragmosis and defence in the casque-headed tree frog *Corythomantis greeningi*. *J Zool* **265**, 1–8.

Kley NJ (2001) Prey transport mechanisms in blindsnakes and the evolution of unilateral feeding systems in snakes. *Am Zool* **41**, 1321–1337.

Kley NJ (2006) Morphology of the lower jaw and suspensorium in the Texas blindsnake, *Leptotyphlops dulcis* (Scolecophidia: Leptotyphlopidae). *J Morphol* **267**, 494–515.

Kraus F (2017) New species of blindsnakes (Squamata: Gerrhopilidae) from the offshore islands of Papua New Guinea. *Zootaxa* **4299**, 75–94.

Lee MSY, Scanlon JD (2002) Snake phylogeny based on osteology, soft anatomy and ecology. *Biol Rev* **77**, 333–401.

Lee MSY, Hugall AF, Lawson R, et al. (2007) Phylogeny of snakes (Serpentes): combining morphological and molecular data in likelihood, Bayesian and parsimony analyses. *Syst Biodivers* **5**, 371–389.

List JC (1966) Comparative osteology of the snake families Typhlopidae and Leptotyphlopidae. *Illinois Biol Monogr* **36**, 1–112.

Macalister A (1875) A monograph of the anatomy of *Chlamydophorus truncatus* (Harlan), with notes on the structure of other species of Edentata. *Trans R Ir Acad* **25**, 219–278.

Macey JR, Verma A (1997) Homology in phylogenetic analysis: alignment of transfer RNA genes and the phylogenetic position of snakes. *Mol Phylogenet Evol* **7**, 272–279.

McDowell SB (2008) The skull of Serpentes. In: *Biology of the Reptilia. Volume 21. Morphology I. The Skull and Appendicular Locomotor Apparatus of Lepidosauria*. (eds Gans C, Gaunt AS, Adler K), pp. 467–620. Ithaca, NY: Society for the Study of Amphibians and Reptiles.

Mead JI (2013) Scolecophidia (Serpentes) of the late oligocene and early miocene, North America, and a fossil history overview. *Geobios* **46**, 225–231.

Miralles A, Marin J, Markus D, et al. (2018) Molecular evidence for the paraphyly of Scolecophidia and its evolutionary implications. *J Evol Biol* **31**, 1782–1793.

Oelrich TM (1956) The anatomy of the head of *Ctenosaura pectinata* (Iguanidae). *Miscellaneous Publications, Museum of Zoology, University of Michigan* **94**, 1–122.

Palci A, Lee MSY, Hutchinson MN (2016) Patterns of postnatal ontogeny of the skull and lower jaw of snakes as revealed by micro-CT scan data and three-dimensional geometric morphometrics. *J Anat* **229**, 723–754.

Parker HW, Grandison AGC (1977) *Snakes — A Natural History*. London: British Museum of Natural History.

Pyron RA, Burbrink FT, Wiens JJ (2013a) A phylogeny and revised classification of Squamata, including 4161 species of lizards and snakes. *BMC Evol Biol* **13**, 93.

Pyron RA, Kandambi HKD, Hendry CR, et al. (2013b) Genus-level phylogeny of snakes reveals the origins of species richness in Sri Lanka. *Mol Phylogenet Evol* **66**, 969–978.

Reeder TW, Townsend TM, Mulcahy DG, et al. (2015) Integrated analyses resolve conflicts over squamate reptile phylogeny and reveal unexpected placements for fossil taxa. *PLoS One* **10**, e0118199.

Rieppel O (1979) The braincase of *Typhlops* and *Leptotyphlops* (Reptilia: Serpentes). *Zool J Linn Soc* **65**, 161–176.

Rieppel O (1988) A review of the origin of snakes. In: *Evolutionary Biology*. (eds Hecht MK, Wallace B, Prance GT), pp. 37–130. New York: Plenum.

Rieppel O, Kley NJ, Maisano JA (2009) Morphology of the skull of the white-nosed blindsnake, *Liotyphlops albirostris* (Scolecophidia: Anomalepididae). *J Morphol* **270**, 536–557.

Scherz MD, Hawlitschek O, Andreone F, et al. (2017) A review of the taxonomy and osteology of the *Rhombophryne serratopalpebrosa* species group (Anura: Microhylidae) from Madagascar, with comments on the value of volume rendering of micro-CT data to taxonomists. *Zootaxa* **4273**, 301–340.

Stalling D, Westerhoff M, Hege HC (2005) Amira: a highly interactive system for visual data analysis. In: *The Visualization Handbook*. (eds Hansen CD, Johnson CR), pp. 749–770. Oxford: Elsevier Butterworth-Heinemann.

Streicher JW, Wiens JJ (2017) Phylogenomic analyses of more than 4000 nuclear loci resolve the origin of snakes among lizard families. *Biol Let* **13**, 20170393.

Szyndlar Z (1991) A review of neogene and quaternary snakes of central and eastern Europe. Part 1: Scolecophidia, Boidae, Colubrinae. *Estud Geol* **47**, 103–126.

Vidal N, Hedges SB (2002) Higher-level relationships of snakes inferred from four nuclear and mitochondrial genes. *CR Biol* **325**, 977–985.

Vidal N, Hedges SB (2005) The phylogeny of squamate reptiles (lizards, snakes, and amphisbaenians) inferred from nine nuclear protein-coding genes. *CR Biol* **328**, 1000–1008.

Vidal N, Delmas AS, David P, et al. (2007) The phylogeny and classification of caenophidian snakes inferred from seven nuclear protein-coding genes. *CR Biol* **330**, 182–187.

Vidal N, Marin J, Morini M, et al. (2010) Blindsnake evolutionary tree reveals long history on Gondwana. *Biol Let* **6**, 558–561.

Vitt LJ, Caldwell JP (2009) *Herpetology: An Introductory Biology of Amphibians and Reptiles*. Burlington: Academic Press.

Wallach V, Ineich I (1996) Redescription of a rare Malagasy blind snake, *Typhlops grandidieri* Mocquard, with placement in a new genus (Serpentes: Typhlopidae). *J Herpetol* **30**, 367–376.

Webb JK, Shine R (1993) Dietary habits of Australian blindsnakes (Typhlopidae). *Copeia* **1993**, 762–770.

Webb JK, Branch WR, Shine R (2001) Dietary habits and reproductive biology of typhlopid snakes from southern Africa. *J Herpetol* **35**, 558–567.

Wegener JE, Swoboda S, Hawlitschek O, et al. (2013) Morphological variation and taxonomic reassessment of the endemic Malagasy blind snake family Xenotyphlopidae. *Salamandra* **36**, 269–282.

Wheeler WM (1927) Physiognomy of insects. *Q Rev Biol* **2**, 1–36.

Wiens JJ, Kuczynski CA, Smith SA, et al. (2008) Branch length, support, and congruence: testing the phylogenomic approach with 20 nuclear loci in snakes. *Syst Biol* **57**, 420–431.

Young BA, Wallach V (1998) Description of a papillate tactile organ in the Typhlopidae. *S Afr J Zool* **33**, 249–253.

Zheng Y, Wiens JJ (2016) Combining phylogenomic and supermatrix approaches, and a time-calibrated phylogeny for squamate reptiles (lizards and snakes) based on 52 genes and 4162 species. *Mol Phylogenet Evol* **94**, 537–547.

Supporting Information

Additional Supporting Information may be found in the online version of this article:

Fig. S1. PDF-embedded 3D model of the segmented skull of *Xenotyphlops grandidieri* specimen ZSM 2194/2007. Open this PDF in Adobe® Acrobat Reader IX or later, and click on the model to activate it.

Fig. S2. PDF-embedded 3D model of the unsegmented skull of *Xenotyphlops grandidieri* specimen ZSM 2213/2007. Open this PDF in Adobe® Acrobat Reader IX or later, and click on the model to activate it.

Fig. S3. PDF-embedded 3D model of the unsegmented skull of *Xenotyphlops grandidieri* specimen ZSM 2216/2007. Open this PDF in Adobe® Acrobat Reader IX or later, and click on the model to activate it.